

Chapter 2

Cell Volume Regulation Monitored with Combined Epifluorescence and Digital Holographic Microscopy

Nicolas Pavillon and Pierre Marquet

Abstract

Quantitative phase imaging emerged recently as a valuable tool for cell observation, by enabling label-free imaging through the intrinsic phase-contrast provided by transparent living cells, thus greatly simplifying observation protocols. The quantitative phase signal, unlike the one provided by the widely used phase-contrast microscope, can be related to relevant biological indicators including dry mass, cell volume regulation or transmembrane water movements. Here, we present quantitative phase imaging coupled with live fluorescence, making it possible to follow the phase signal in time to monitor the cell volume regulation, an early indicator of cell viability, along with specific information such as intracellular Ca^{2+} imaging with Fura-2 ratiometric fluorescence.

Key words Microscopy, Quantitative phase imaging, Digital holography, Fluorescence, Ca^{2+} imaging, Cell biology, Cell volume regulation

1 Introduction

Phase imaging has been historically one of the first tools available to visualize transparent living cells, since the invention of the phase-contrast microscope in the forties of the last century [1]. Nowadays, a microscope employing phase-contrast or differential interference contrast (DIC) microscopy [2] is a fundamental tool of any wet laboratory, for example to assess cell cultures condition.

Outside routine observation, these tools have then been mostly supplanted by more specific imaging approaches such as staining, which permits to differentiate tissues in histological slides, or functional imaging through fluorescence. There is however a renewed interest for phase imaging in the recent years, thanks to the rapid development of a new type of imaging called quantitative phase microscopy (QPM).

Unlike most microscopy methods which rely on intensity contrast, such as the absorption of a specimen or the emission of a specific fluorophore, phase imaging is based on the measurement of

the variation of a light wave front passing through a specimen, making it sensitive to its refractive index, a physical property intimately linked with the density of intracellular components, but primarily determined by the intracellular protein concentration. One of its main characteristics is that it does not require labeling, making experimental protocols far simpler than for most recent imaging approaches. Another feature worth mentioning is its recording speed capability (10–100 frames per second with standard cameras). On the other hand, the signal it delivers is typically less specific than fluorescence, which can be used for instance with specific chemical bonding dyes, so that its interpretation is more challenging.

It has been demonstrated in the past years that QPM could be used, for example, to monitor cell morphology and life cycle [3, 4], to measure the cell dry mass [5, 6], or to assess cell viability [7, 8]. This chapter discusses a particular application of phase imaging, where it is used in conjunction with wide-field fluorescence [9], in order to obtain, in parallel, the phase information along with specific information from a chosen dye. The fluorophore presented here consists of Fura-2, a ratiometric dye which makes it possible to monitor the concentration of free intracellular Ca^{2+} [10, 11].

1.1 Principle of Quantitative Phase Measurement

While a complete description of the technical aspects involved in the measurement of QPM is beyond the scope of this chapter, it is worthwhile mentioning some fundamental elements. For more details, interested readers can refer to existing reviews mentioning, in particular, the numerous methods allowing to obtain a quantitative phase signal (*see* refs. [12–14]).

In the application presented here, phase imaging is coupled with fluorescence, by employing a spectral separation scheme; this implies that the light used for QPM must not overlap with the excitation and emission bands of the employed fluorophore. For this reason, we focus on QPM with laser light, and more particularly on a technique called off-axis digital holographic microscopy (DHM) [15, 16].

Off-axis DHM is a specific implementation which uses coherent light to generate holograms, from which quantitative phase images can be extracted through numerical reconstruction. Its main feature is a fast imaging capability by enabling phase retrieval with a single hologram. Interested readers can refer to existing literature for a detailed overview of the theoretical steps involved in hologram reconstruction [17, 18]. In this context, the laser light employed for DHM is well defined in the optical spectrum and can be separated from the fluorescence emission, yielding two independent signals [9], as employed in this chapter.

1.2 Phase Signal Interpretation

One key point when employing phase measurement on biological samples such as cells is to interpret the measurement correctly. The phase is essentially proportional to the refractive index of the

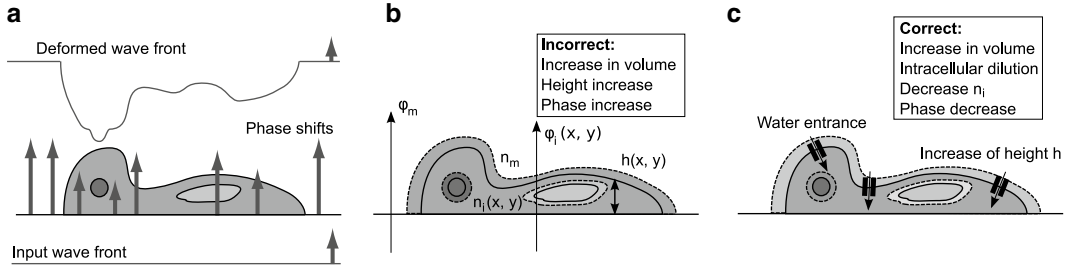


Fig. 1 (a) Schematic representation of the generation of the phase signal, where the input wave front is deformed by the optical density of the different organelles. (b) Naive interpretation of the effect of a cell volume increase on the phase signal, through the increase in height $h(x, y)$. (c) Correct interpretation, when taking into account intracellular dilution during volume increase

intracellular content of a cell and to its thickness. The generation of a phase wave front is depicted in Fig. 1a, where the light of an input planar wave front passing through a cell is deformed as it is retarded by the cellular content which has a larger optical density (refractive index) than the extracellular medium. Organelles can be identified by an additional phase shift, being either positive or negative depending on their refractive index.

Mathematically, the phase signal can be expressed as

$$\begin{aligned} \Delta\varphi(x, y) &= \varphi_i(x, y) - \varphi_{\text{ref}} \\ &= \frac{2\pi}{\lambda} (n_i(x, y) - n_m) h(x, y), \end{aligned} \quad (1)$$

where $\varphi_i(x, y)$ is the phase shift at a location in the cell, φ_{ref} is the phase shift outside the cell (background signal), λ is the DHM laser wavelength, $n_i(x, y)$ is the average refractive index value along the optical axis, n_m is the refractive index of the perfusion medium, and $h(x, y)$ is the cell height at a given location, as represented in Fig. 1b.

The phase signal can be counter-intuitive at first sight, since a cell volume increase, as depicted in Fig. 1b, leading to an increase of the height $h(x, y)$, does not correspond to a phase increase, as Eq.(1) could indicate. This is due to the fact that through cell volume homeostasis, a volume increase is concomitant with water entry through various membrane pathways, as depicted in Fig. 1c, which implies an intracellular content dilution, and consequent decrease of the refractive index $n_i(x, y)$ and phase. In the case of cellular bodies, the changes in refractive index $n_i(x, y)$ are indeed more significant than the height $h(x, y)$ on the phase signal. This is due to the fact that a change in height, which purely modifies the respective contributions of n_i and n_m , has a low influence as the intracellular n_i is classically close to the one of the medium n_m .

The phase signal should thus be understood generally as an indication of intracellular dilution for proper interpretation.

In this fashion, the phase signal can be used as an indicator of cell volume regulation (CVR), which is related to the transmembrane water movements occurring for instance during ionic homeostasis [7, 19]. In this context, the CVR can be employed as an early indicator of cell viability [20], since a prolonged dysregulation is known to trigger several cellular death pathways [21].

1.3 Ratiometric Fluorescence

Live fluorescence can be employed to monitor specific biological parameters. In this chapter, we employ intracellular fluorescent probes [22] to measure the free Ca^{2+} concentration. Ionic concentration dyes are based on the activation of the fluorophore upon bonding with the investigated ion, so that the intensity of the measured fluorescence signal depends on the amount of ions attached to fluorescent molecules, in function of the dissociation constant of the bonding chemical reaction [11].

Several dyes denoted as ratiometric have the property of changing their absorption spectrum, so that their maximum of absorption shifts in wavelength upon bonding with their affinity ion [10]. In this case, the signal can be calculated as a ratio between two excitation wavelengths as

$$R = \frac{F_{\lambda_1}}{F_{\lambda_2}}, \quad (2)$$

where F_{λ_1} is the fluorescent signal at the first excitation wavelength, and F_{λ_2} at the second. A ratiometric measurement presents several advantages, such as making the final measurement independent of the intracellular concentration of fluorophore molecules, and more robust towards photobleaching.

Fura-2 is a ratiometric fluorophore sensitive to $[\text{Ca}^{2+}]$ at low concentrations (typically 100 nM). It is excited in the ultraviolet with typical wavelengths $\lambda_1 = 340$ nm and $\lambda_2 = 380$ nm, and emits light in the green region.

2 Materials

On a general point of view, QPM is characterized by rather simple protocols, thanks to its label-free imaging capability. This implies that nearly any sample can be imaged directly out of the cell incubator. However, several steps described in this chapter can greatly increase the image and signal quality.

Furthermore, it should be reminded that the phase signal can be indiscriminately coupled with any fluorophore, as long as the DHM wavelength laser does not overlap with the excitation and emission spectra of the dye. The materials and methods provided here for fluorescence, namely intracellular $[\text{Ca}^{2+}]$ dynamics monitored with a ratiometric probe, could thus be interchanged with other standard protocols for other fluorophores, in order to

observe another cell property along with the phase signal (*see Note 1*). Several examples employing other fluorophores such as Fluo-4 or propidium iodide can be found in the literature [23].

Similarly, the excitation solution provided here is meant for observation of the response of neuronal cells under glutamate perfusion, but the protocol can be modified in order to observe other types of responses.

While the protocols below assume the type of equipment detailed in the following, they should still be valid or easily adaptable for different configurations.

Unless specified otherwise, all operations are supposed to be performed at room temperature. For the preparation of solutions, employ ultrapure sterilized water. For each employed chemical, follow the handling instructions provided by the manufacturer.

2.1 Equipment

1. DHM T1000[®] microscope (Lyncée Tec, Lausanne, Switzerland).
2. Epi-fluorescence module for DHM T1000[®] [9] (Lyncée Tec).
3. Koala[®] software (Lyncée Tec).
4. MetaFluor[®] software (Molecular Devices, Sunnyvale, CA).

2.2 Cell Culture Handling

1. Poly-L-ornithine (PLO) pre-coated microscopy glass coverslips (Sigma Chemicals, St. Louis, MO). *See Notes 2 and 3.*
2. Six- or twenty-four-well plates.
3. Perfusion chamber. *See Note 4.*
4. Perfusion system.

2.3 Solutions

1. L-glutamate stock solution: dilute a vial of L-glutamate (Tocris Bioscience, Bristol, UK) to 25 mM with ultrapure water. Store in small aliquots at -20°C .
2. Perfusion solution: 140 mM NaCl, 3 mM KCl, 3 mM CaCl_2 , 2 mM MgCl_2 , 5 mM glucose, 10 mM HEPES. Dilute in ultrapure water (75 % of the final volume). Then, adjust the pH to 7.3 by gradually adding 1 M NaOH. Adjust finally the volume to the desired quantity (*see Notes 5 and 6*). If not used at once, store at 4°C .
3. Excitatory solution: right before the experiment, dilute the L-glutamate stock solution to 30 μM in a small volume (typically 10 mL) of the perfusion solution.

2.4 Loading of Calcium Indicator

1. Calcium indicator stock solution: dilute one vial of Fura-2 acetoxyethyl ester (AM) salt (Molecular Probes[®], Life Technologies[™], Carlsbad, CA) at 2 mM with dimethyl sulfoxide (DMSO). Store at -20°C and protect from light.
2. Loading solution: dilute the calcium indicator stock solution at 4 μM in 1 mL of perfusion solution.

3. Place cells in a 35 mm Petri dish with the loading solution and incubate at 37 °C for 30 min.
4. Wash 2–3 times with the perfusion solution to remove the loading solution and incubate at 37 °C for 10 min to ensure full de-esterification of the dye before observation.

3 Methods

The method described below consists of two main steps, first being the measurement itself, where holograms and fluorescence images are acquired in a given set of conditions. The second step consists in the data treatment, in order to extract the signals from the measurements. In case of fluorescence and DHM measurements, the offline processing of the data is also of key importance, as careless treatment can lead to incorrect results, making it a step of similar importance to the measurement itself to derive reliable results.

3.1 Measurements

1. Mount cells in the perfusion chamber (*see Note 7*) and place them under the microscope (*see Note 8*).
2. Connect the chamber to the perfusion system. The perfusion chamber and system must ensure rapid delivery and exchange of the perfusion solutions. Start flux with the perfusion solution. *See Note 9*.
3. Select a magnification of 10–20× (*see Notes 10 and 11*), and choose a zone of interest (*see Note 12*) to be measured. The field of view should contain enough cells for imaging, but avoid too dense regions, as cells may be difficult to identify afterwards.
4. Open the fluorescence lamp shutter, and focus the fluorescence image. It is important to ensure a proper focus for a good fluorescence signal (*see Note 10*), but this should be performed rapidly, to avoid bleaching of the fluorophore (*see Note 13*).
5. Close the fluorescence lamp shutter, and set it to open only during image acquisition.
6. Set the fluorescence acquisition to successive excitation at $\lambda_1 = 340$ nm and $\lambda_2 = 380$ nm (*see Note 14*).
7. Start acquisition of both holograms (with the Koala® software) and fluorescence images (with the MetaFluor® software) in order to record a baseline of at least 5–10 min, with an acquisition rate of 0.5 Hz in fluorescence, and typically 1–5 Hz with DHM (*see Note 15*).
8. After baseline measurement, increase the acquisition rate of fluorescence to 2 Hz to ensure being able to follow the rapid $[Ca^{2+}]$ rise, and perfuse the excitatory solution for 30 s.

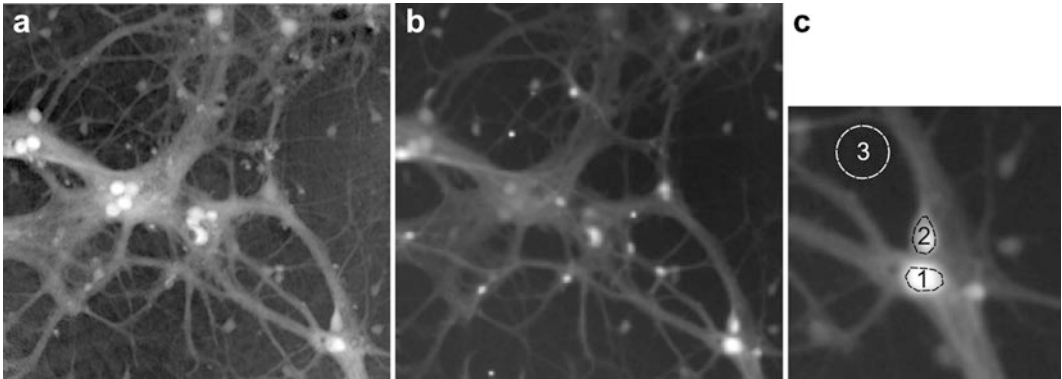


Fig. 2 Typical images of hippocampal neuron cells in culture measured with (a) label-free quantitative unwrapped phase, representing a dynamic range of $[0, 9.6]$ radians and (b) Fura-2 fluorescence, excited at 380 nm. The field of view represents a region of $360 \times 350 \mu\text{m}$. (c) Illustration of the selection of 2 cell soma (1, 2) and a background region (3) for computation of the average fluorescence intensity

9. After calcium reached its maximum, reduce the frame rate of fluorescence back to 0.5 Hz.
10. Continue acquisition to follow the rest of the response, during typically 30–40 min.
11. If required, perform a second excitation, otherwise terminate the experiment.

An example of typical measurements taken with the protocol given above is shown in Fig. 2, with the quantitative phase image reconstructed from the hologram (*see* Fig. 2a) and the Fura-2 fluorescence image at 380 nm (*see* Fig. 2b).

One can appreciate the difference of contrast between the two images, where all neurons can be easily identified in phase, while their visibility in fluorescence depends on the intracellular Ca^{2+} concentration, but also on the fluorescent dye loading efficiency for each cell.

3.2 Treatment of Data

1. With fluorescence images use the MetaFluor® software. Compute the mean fluorescence intensity value of the measured cells by selecting the soma. Ensure that the selection region is well placed within the cell in order to avoid signal disruption from pixels outside the cell (*see* Fig. 2c). Also select a background region outside any cell (*see* Note 16).
2. Extract the temporal fluorescence signal on the chosen regions by running through all measured images.
3. Subtract the background signal from the different cell signals, in order to suppress the background fluorescence and potential temporal drifts. For a ratiometric measurements, this implies to make the subtraction on both measured wavelengths.

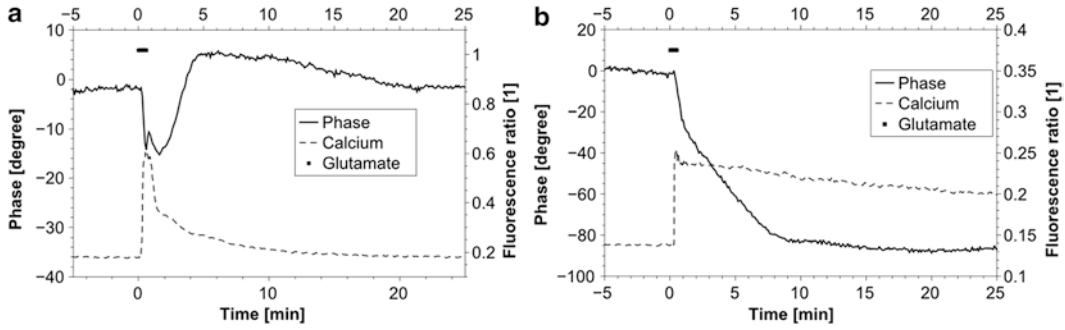


Fig. 3 Typical glutamate-mediated responses obtained by monitoring quantitative phase and Fura-2 fluorescence on neuron cells soma. **(a)** Physiological response, characterized by transient signals which are rapidly regulated. **(b)** Pathological response, associated with a dysregulation in both phase (indicative of an absence of CVR) and $[Ca^{2+}]$

4. Compute the ratiometric signal by dividing the two signals according to Eq. (2).
5. From the acquired holograms, reconstruct the phase signals with the Koala[®] software (*see* **Note 17**).
6. Perform a similar analysis on phase images by repeating points 1–3, i.e., by selecting similar regions on the cells and a background signal, and subtracting the background.
7. The two signals can be compared by matching the two temporal axes, as shown for example in Fig. 3.

An example of typical measurements as obtained from the protocol given above is provided in Fig. 3, where the temporal signals of phase and ratiometric Fura-2 are presented for both a physiological response (*see* Fig. 3a) and a pathological one (*see* Fig. 3b). Glutamate, the main excitatory neurotransmitter in the brain, induces an early response characterized by an intracellular increase of Na^+ and Ca^{2+} , as well as a neuronal swelling resulting from a transmembrane influx of water associated with the ions entrance for osmotic reasons. The physiological case is characterized by a transient phase decrease, indicative of a cell swelling, which is regulated in the minutes following the stimulation. This decrease is concomitant with the intracellular $[Ca^{2+}]$ increase, which rapidly returns to basal levels. On the other hand, the pathological response is characterized by an irreversible decrease in phase and rise in $[Ca^{2+}]$ levels, which are not regulated. This absence of CVR was shown to be an early marker of the subsequently neuronal death [7], linked here with the known toxicity of intracellular $[Ca^{2+}]$ dysregulation during glutamate stimulation [24].

4 Notes

1. As the principle for combined imaging presented in this chapter only relies on the absence of overlap between the laser light of DHM and the excitation/emission spectra of the fluorophore, nearly any dye could be employed with a similar protocol. Changing the dye thus essentially corresponds to change the filter cube, as in any standard fluorescence microscope. As an example, the laser wavelength used in this chapter is 680 nm, so that any dye emitting in the blue, green, yellow, or orange could be used. Additionally, the DHM laser light is not fixed, so that another laser could also be employed to extend the usable range of fluorophores.
2. As phase is sensitive to the surface quality of the different interfaces, glass substrates are usually preferred to ensure the best signal stability. Plastic can indeed have scratches which can appear in the image, and add noise to the signal. For this reason, in case Petri dishes are used for observation, it is usually preferable to use glass-bottom dishes, or to culture cells on microscopy slides, which can be stored in Petri dishes or well plates during cell culture.
3. The protocol described in this chapter is exemplified with measurements on astrocytes-neurons cocultures. PLO is known to provide a better adherence for astrocytes, but the coating should be adapted depending on the cell type, such as poly-L-lysine or collagen as a replacement for PLO.
4. It is assumed here that a closed perfusion chamber is used, which implies that both interfaces in the sample are made of glass. This ensures the best results for phase measurements, and a better control of the flux during perfusion. The closed perfusion chamber can however be replaced with an open chamber such as a Petri dish. In this case, the air-liquid interface may vary during the experiment and thus induce additional noise, which may have to be compensated with additional procedures [18, 25].
5. It has to be noted that it is also possible to perform DHM measurements in other solutions than isotonic ones, such as growth medium. However, fluorescence requires to avoid media with dyes such as phenol red, which can cause autofluorescence. Furthermore, isotonic solutions have a lower refractive index, so that a slight improvement in contrast may be observed also in phase.
6. As the phase is sensitive to volume changes and transmembrane water movements, it is important to ensure that the osmolarity of the perfusion solution is close to the one of the growth medium, in order to avoid hyper- or hypotonic shocks which could disrupt the baseline of the measurement.

7. Phase imaging is sensitive to surface quality, so that cleaning the bottom of the dish or of the coverslip with alcohol before the experiment can tremendously improve the image and signal quality by removing potential dust or dirt resulting from cell growth or previous manipulation.
8. It is good practice to turn on the different devices of the microscope a while before the experiment (at least 30 min), to let the light sources stabilize to ensure constant illumination, and let the whole setup come at functioning temperature to avoid mechanical drifts.
9. It is very important to avoid having any bubble in the perfusion system, as even small bubbles in tubes can gather while passing in the flux, and eventually wash cells when passing in the perfusion chamber.
10. A magnification which is too small makes it difficult to identify the cell soma during the processing of the experiment, and a too high one significantly reduces the field of view, so that only a few cells can be measured during the experiment. A magnification between $10\times$ and $20\times$ is a good compromise in case of neurons, but may have to be adjusted depending on the cell size and distribution.
11. High magnifications have the issue of inducing a short depth of field, so that small mechanical drifts can lead to strongly defocused images, which severely degrade the fluorescence signal. In this case, mechanical refocus during the experiment may be necessary to ensure a reliable fluorescence signal.
12. It is usually very useful to ensure that a part of the measured field of view is free of cells, in order to provide a region on which a background signal can be recorded, for suppressing the autofluorescence and stray light contribution in fluorescence, and for retaining a reliable phase reference to ensure measurement stability.
13. The mechanical focus should be adjusted according to the fluorescence image, as DHM possesses a feature of digital focusing [26], so that cells can be brought into focus during off-line DHM reconstruction, making it possible to avoid perturbing the experiment with manual refocusing.
14. The excitation wavelengths for Fura-2 are classically chosen at $\lambda_1 = 340$ nm and $\lambda_2 = 380$ nm, corresponding to the maximum absorption wavelengths of respectively the bonded and free form of the molecule. However, an excitation as low as 340 nm can require specific optical components to ensure a sufficient transmittance, which are not always available. For this reason, it is also possible to use $\lambda_1 = 360$ nm, which corresponds to the isosbestic point of Fura-2—the absorption point which stays constant upon bonding with Ca^{2+} —to ensure a better transmittance of the excitation light.

15. The temporal resolution of the phase measurement can be set at will, as there is no concern about phototoxicity, bleaching or too long exposure times. The usual practical limit can be determined in order to adequately sample the studied phenomenon without employing too much space on hard drives. In contrast, acquisition of fluorescence images must be limited in order to avoid too much bleaching. For this reason, a shutter system is also necessary to expose cells only during image acquisition.
16. It can happen that cells move during the measurement. It may therefore be necessary to adjust the regions throughout the treatment of the measurements, or track the cell soma over all images in order to retrieve a proper signal.
17. Phase shifts induced by cells can be rather large, and go beyond the accessible dynamic range of the phase signal, which is bound between $[0, 2\pi]$ radians. It may thus be necessary to employ unwrapping procedures to obtain a continuous signal. There are several methods for unwrapping phase signals, but typical examples of use and implementations can be found in refs. [27, 28].

Acknowledgements

This research was supported by the Swiss National Science Foundation grant #CR32I3-132993 and by the Commission for Technology and Innovation (CTI/KTI) project #9389.1.

References

1. Zernike F (1955) How I discovered phase contrast. *Science* 121:345–349
2. Allen R, David G, Nomarski G (1969) The Zeiss-Nomarski differential interference equipment for transmitted-light microscopy. *Z Wiss Mikrosk* 69:193–221
3. Rappaz B, Marquet P, Cuche E et al (2005) Measurement of the integral refractive index and dynamic cell morphometry of living cells with digital holographic microscopy. *Opt Express* 13:9361–9373
4. Girshovitz P, Shaked NT (2012) Generalized cell morphological parameters based on interferometric phase microscopy and their application to cell life cycle characterization. *Biomed Opt Express* 3:1757–1773
5. Rappaz B, Cano E, Colomb T et al (2009) Noninvasive characterization of the fission yeast cell cycle by monitoring dry mass with digital holographic microscopy. *J Biomed Opt* 14:034049
6. Mir M, Wang Z, Shen Z et al (2011) Optical measurement of cycle-dependent cell growth. *Proc Natl Acad Sci U S A* 108:13124–13129
7. Pavillon N, Kühn J, Moratal C et al (2012) Early cell death detection with digital holographic microscopy. *PLoS ONE* 7:e30912
8. Khmaladze A, Matz RL, Epstein T et al (2012) Cell volume changes during apoptosis monitored in real time using digital holographic microscopy. *J Struct Biol* 178:270–278
9. Pavillon N, Benke A, Boss D et al (2010) Cell morphology and intracellular ionic homeostasis explored with a multimodal approach combining epifluorescence and digital holographic microscopy. *J Biophotonics* 3:432–436
10. Grynkiewicz G, Poenie M, Tsien R (1985) A new generation of Ca^{2+} indicators with greatly improved fluorescence properties. *J Biol Chem* 260:3440–3450
11. Tsien RY (1989) Fluorescent probes of cell signaling. *Annu Rev Neurosci* 12:227–253

12. Kreis T (2005) Handbook of holographic interferometry. Wiley-VCH, Weinheim, Germany
13. Popescu G (2011) Quantitative phase imaging of cells and tissues. McGraw-Hill, New York, NY
14. Magistretti P, Marquet P, Depeursinge C (2013) Neural cell dynamics explored with digital holographic microscopy. *Annu Rev Biomed Eng* 15:407–431
15. Cuche E, Marquet P, Depeursinge C (1999) Simultaneous amplitude-contrast and quantitative phase-contrast microscopy by numerical reconstruction of Fresnel off-axis holograms. *Appl Opt* 38:6994–7001
16. Marquet P, Rappaz B, Magistretti P et al (2005) Digital holographic microscopy: A noninvasive contrast imaging technique allowing quantitative visualization of living cells with subwavelength axial accuracy. *Opt Lett* 30:468–470
17. Montfort F, Charrière F, Colomb T et al (2006) Purely numerical compensation for microscope objective phase curvature in digital holographic microscopy: Influence of digital phase mask position. *J Opt Soc Am A* 23: 2944–2953
18. Colomb T, Kühn J, Charrière F et al (2006) Total aberrations compensation in digital holographic microscopy with a reference conjugated hologram. *Opt Express* 14: 4300–4306
19. Jourdain P, Pavillon N, Moratal C et al (2011) Determination of transmembrane water fluxes in neurons elicited by glutamate ionotropic receptors and by the co-transporters KCC2 and NKCC1: a digital holographic microscopy study. *J Neurosci* 31:11846–11854
20. Hoffmann E, Lambert I, Pedersen S (2009) Physiology of cell volume regulation in vertebrates. *Physiol Rev* 89:193–277
21. Chen M, Sepramaniam S, Armugam A et al (2008) Water and ion channels: crucial in the initiation and progression of apoptosis in central nervous system? *Curr Neuropharmacol* 6:102–116
22. Tsien RY (1981) A non-disruptive technique for loading calcium buffers and indicators into cells. *Nature* 290:527–528
23. Pavillon N (2011) Cellular dynamics and three-dimensional refractive index distribution studied with quantitative phase imaging. Ph.D. thesis no 5100, Ecole Polytechnique Fédérale de Lausanne
24. Stout A, Raphael H, Kanterewicz B et al (1998) Glutamate-induced neuron death requires mitochondrial calcium uptake. *Nat Neurosci* 1:366–373
25. Colomb T, Montfort F, Kühn J et al (2006) Numerical parametric lens for shifting, magnification, and complete aberration compensation in digital holographic microscopy. *J Opt Soc Am A* 23:3177–3190
26. Langehanenberg P, Kemper B, Dirksen D et al (2008) Autofocusing in digital holographic phase contrast microscopy on pure phase objects for live cell imaging. *Appl Opt* 47: D176–D182
27. Takajo H, Takahashi T (1988) Noniterative method for obtaining the exact solution for the normal equation in least-squares phase estimation from the phase difference. *J Opt Soc Am A* 5:1818–1827
28. Su X, Chen W (2004) Reliability-guided phase unwrapping algorithm: a review. *Optic Laser Eng* 42:245–261

Neuronal Cell Death

Methods and Protocols

Lossi, L.; Merighi, A. (Eds.)

2015, XIV, 396 p. 82 illus., 48 illus. in color., Hardcover

ISBN: 978-1-4939-2151-5

A product of Humana Press